WATER RESOURCES RESEARCH, VOL. 49, 1–14, doi:10.1002/wrcr.20089, 2013

Modeling increases in snowmelt yield and desynchronization resulting from forest gap-thinning treatments in a northern mountain headwater basin[1]

C. R. Ellis,[1,2] J. W. Pomeroy,[1] and T. E. Link[3]

Received 4 March 2012; revised 14 December 2012; accepted 5 January 2013.

[1] A physically based model built upon extensive field observations of radiation dynamics and snow processes in cold regions forest environments was used to investigate the impacts of prescribed forest gap-thinning treatments on spring snowmelt in a small Saskatchewan River headwater basin of the Canadian Rocky Mountains. Both field observations and model simulations showed that snow accumulations in small clear-cut gaps was roughly double those under intact forest cover due to sublimation losses from the canopy. Consequently, mountain forests thinned with small clear-cut gaps resulted in a substantial increase in the magnitude of spring snowmelt. However, the impact of forest thinning on the timing of snowmelt was highly dependent on slope orientation; thinning accelerated snowmelt on south facing slopes primarily through enhanced shortwave radiation, but retarded snowmelt on north facing slopes primarily through reduced incoming longwave radiation. As a result, thinning treatments across opposing north facing and south facing mountain slopes acted to substantially expand the spring melt period in the basin, and illustrated the important hydrological control imparted by intact forest cover through its synchronization of snowmelt across complex terrain. A sensitivity analysis of snowmelt timing to varying spring meteorological conditions strongly suggests that shifts in spring snowmelt runoff from similar forest thinning treatments in mountain regions will depend on the slope and aspect at which they occur in combination with the seasonal timing of snowmelt resulting from latitude-controlled solar elevation effects.

Citation: Ellis, C. R., J. W. Pomeroy, and T. E. Link (2013), Modeling increases in snowmelt yield and desynchronization resulting from forest gap-thinning treatments in a northern mountain headwater basin, *Water Resour. Res.*, *49*, doi:10.1002/wrcr.20089.

1. Introduction

[2] In western and northern North America, the majority of river flows are generated from snowmelt, much of which originates in complex mountain landscapes [*Eschner et al*., 1969; *Gray and Landine*, 1988; *Mote et al*., 2005; *Woo*, 2008], providing a vital water supply to the Peace-Athabasca-Mackenzie, Columbia, Colorado, Fraser, Saskatchewan-Nelson, Churchill, and Missouri Rivers [*Marks and Winstral*, 2001]. Northern mountains have extensive evergreen needleleaf forests, which strongly influence snowmelt runoff due to impacts both on snow accumulation [*Jeffery*, 1965; *Lundberg and Halldin*, 1994; *Pomeroy et al*., 2002] and snowmelt timing [*Metcalfe and Buttle*, 1995; *Davis et al*., 1997; *Pomeroy and Granger*, 1997; *Hardy et al*., 1998]. Mountain streamflow is under ever-increasing demand to satisfy the rapidly expanding agricultural, industrial, and municipal water needs of western North America [*Martz et al*., 2007], which threaten to limit the instream flows necessary to maintain aquatic ecological health and recreational opportunities. Forest cover, snow conditions, and climate are changing rapidly across the region [*Stewart et al*., 1998; *Nash and Johnson*, 1996; *Mote et al*., 2005; *Barnett et al*., 2008; *Knowles et al.,* 2006]. Given the complex interaction of climate, topography, and vegetation cover in mountain forests, an enhanced understanding of snow processes in these environments is a critical knowledge gap that needs addressing in order to improve the understanding and prediction of how specific changes in vegetation may affect snow dynamics and river flows from cold mountain regions.

[3] Changes in forest cover by either natural or anthropogenic agents may substantially alter the hydrological response of mountain basins [*Troendle and Leaf*, 1980; *Storck et al*., 1998]. However, comprehensive evaluation of the hydrological impacts caused by forest changes is challenging due to the complexity of water flow pathways through natural systems. One commonly employed approach to assess the hydrological impacts from forest cover changes are paired basin experiments, for which the

[1]Centre for Hydrology, University of Saskatchewan, Saskatoon, Saskatchewan, Canada.
[2]Now at Silvatech Consulting Group, Salmon Arm, British Columbia, Canada.
[3]College of Natural Resources, University of Idaho, Moscow, Idaho, USA.

Corresponding author: C. R. Ellis, Centre for Hydrology, University of Saskatchewan, 117 Science Place, Saskatoon, SK, S7N 5C8, Canada. (cre152@mail.usask.ca)

0043-1397/13/10.1002/wrcr.20089

hydrological response from a treated basin is assessed relative to an untreated control. However, insight into the response of specific hydrological processes from such assessments is severely limited due to the logistical challenges in obtaining comprehensive data sets of the relevant hydrological variables over sufficiently long time periods. Another major drawback of such studies involves the differences in hydrological characteristics that naturally exist between even seemingly similar basins, which cast uncertainty in transferring experimental results to other basins.

[4] An alternative approach to empirical paired basin studies is the application of physically based models. With rigorous evaluation of the algorithms describing hydrometeorological processes and meaningful description of the physical environment through specified parameters, these models may be employed to assess the hydrological response brought about by land-use changes such as deforestation or reforestation [*Pomeroy et al*., 1999, 2012]. This is the approach of the Cold Regions Hydrological Modeling (CRHM) platform [*Pomeroy et al*., 2007] and its component process-based modules. Recent evaluations of CRHM have included its forest hydrometeorological modules, which demonstrated an effective representation of snow processes in cold regions needleleaf forest environments [*Ellis et al*., 2010]. The deterministic nature of CRHM is advantageous in terms of allowing a direct assessment of how forest cover changes may impact various snow processes by its ability to output detailed mass and energy balance variables. Spatial heterogeneity of cover and meteorological conditions across a basin are accounted for in CRHM through the designation of separate hydrological response units (HRUs) by the user.

[5] The hypothesis that forest thinning in the form of small gaps acts to retard spring snowmelt follows from *Church's* [1912] assertion that such openings represent the ideal forest structure for snow conservation by promoting snow accumulation sheltered from irradiance (i.e., radiation incident to surface) and turbulent energy exchanges. In terms of snow accumulation, this premise has been largely supported by field observations, with substantially deeper accumulations reported in forest gaps relative to that in adjacent forests [*Golding and Swanson*, 1978; *Gary*, 1980; *Troendle and Leaf*, 1981]. Deeper snow accumulations in forest gaps have been largely attributed to the elimination of canopy snow sublimation losses and the suppression of surface snow sublimation by wind-sheltering from the surrounding remnant forest [*Pomeroy and Gray*, 1995; *Pomeroy et al*., 2002]. In contrast, more conflicting results have been reported regarding the impacts of forest cover on snowmelt timing, as snowmelt in forest gaps has been observed occurring earlier relative to forest snowmelt in Colorado [*Gary and Troendle*, 1982], while *Golding and Swanson* [1978, 1986] and *Swanson et al*. [1986] found substantial snowmelt delays in forest gaps compared to undisturbed Alberta forests. The variable nature of snowmelt in forest gaps was further revealed by *Berry and Rothwell* [1992] who related the rate of snowmelt in forest gaps to their opening size, with more rapid snowmelt occurring in progressively more open gaps.

[6] In general, the large range of snowmelt rates in forest gaps has been attributed to the differing degrees to which snowcover is shaded from shortwave irradiance as produced by varying combinations of gap opening size, topographic orientation, and latitude. The dominant role of radiation in controlling melt rates in Canadian Rocky Mountain forest environments has been confirmed by *Burles and Boon* [2011] as well as by the detailed field measurements reported by *Helgason and Pomeroy* [2012] who revealed that turbulent exchanges provided only modest contributions to total snowmelt energy even in large forest gaps with extended wind fetches. More recent investigations of radiation dynamics in forest gaps have emphasized the role of both shortwave and longwave exchanges in determining total radiation to snowcover [e.g., *Bernier and Swanson*, 1993; *Sicart et al*., 2004]. Detailed field measurements and modeling of shortwave and longwave radiation dynamics by *Lawler and Link* [2011] demonstrated that radiation to snowcover in forest gaps on level terrain at $\sim 47^{\circ}$N latitude may be greater or less than to forest covered or open-site snow depending on solar elevation angle. However, current understanding how forest gaps control radiation to snowcover is even more limited in mountain environments where the combination of forest cover and complex topography create a high degree of spatial variation in shortwave and longwave surface fluxes [*Ellis et al*., 2011].

[7] Detailed field measurements have been used to advance the understanding of processes governing radiation to forest snow and the development of physically based algorithms designed to simulate the impacts of changing canopy structure on snowmelt energetic [e.g., *Pomeroy et al*., 2012; *Fang et al*., 2012]. With their coupling to hydrological models of a similar physically based approach, it is expected these algorithms will provide an improved model representation of the hydrometeorological processes governing how forest cover changes alter the hydrological response of a site and the sensitivity to changing boundary and initial conditions [*Pomeroy et al*., 2005, 2007]. To this end, section 3 of this paper outlines a simple model to determine irradiance in open and forested mountain sites [*Ellis*, 2011], which is extended to describe irradiance in forest gaps of varying dimension based on the procedure by *Lawler and Link* [2011].

[8] The primary objective of this paper is to illustrate the potential effects forest cover changes in the form of prescribed gap-thinning treatments have on the snowmelt response of northern mountain basins. This is accomplished by simulating the shifts in snow accumulation and melt timing produced by the introduction of small canopy gaps in forests on differing slopes and aspects. Simulations are made using the forest-snow process modules in CRHM, which are evaluated against field observations of snow accumulation and melt in the patterned forest gap-thinning treatments established along the upper reaches of the Marmot Creek Research Basin (MCRB) in the Canadian Rocky Mountains. These results are further extended by applying the model to examine how forest gaps impact snowmelt under a wider range of meteorological conditions and basin topographic orientations. Results are likely to help guide hydrological models that operate at the watershed scale in how to provide a better representation of how smaller field-scale forest structures, such as small gap clear-cuts, impact the snow hydrology of mountain basins. Ultimately, insight from this exercise is expected to advance the understanding

of how mountain topography influences the snowmelt response from prescribed forest cutting treatments across mountain regions, and assist watershed and water managers in anticipating how forest cover changes may impact the yield and timing of stream flows derived from spring mountain snowmelt.

2. Forest Harvesting Treatments at MCRB

[9] Initiated in the 1970s as part of the Eastern Slopes Alberta Watershed Research Program [*Beckstead and Veldman*, 1985], extensive prescribed forest harvesting treatments were carried out in the MCRB to assess the potential impacts of large-scale forest cover changes on the snow hydrology of a mountain headwater basin. At the MCRB, forest harvesting was completed in two main treatments: the first establishing six large forest clear-cuts (3–13 ha) in the Cabin Creek subbasin starting in 1974, followed by a forest gap-thinning treatment consisting of 2103 small canopy circular gaps cut along the opposing north facing and south facing slopes of the Twin Creek tributaries through 1977–1979 (Figure 1). In the gap-thinning treatment, the small circular gap openings were spatially positioned to one another forming a honeycomb-like pattern within forest cover, of which the individual gap diameters ranged from ¾ to 1¼ of the surrounding forest height. In general, the intent of the large clear-cutting treatment was to evaluate the potential for increasing total basin snow accumulation and subsequent spring water yield by reducing snow interception losses from the canopy. Although the impacts on total water yield were also of interest with the Twin Creek forest gap-thinning treatment, of particular focus in this subbasin was the prospect of promoting later-season streamflow by delaying snowmelt [*Golding and Swanson*, 1986].

3. Simulation of Irradiance to Mountain Snowcover

3.1. Irradiance to Open Snowcover

[10] At an open site with level topography, all-wave irradiance to snowcover (R_o) is given by the sum of atmospheric (i.e., reference) shortwave irradiance (K_o) and longwave irradiance (L_o) fluxes (all radiation fluxes in W m^{-2} or MJ m^{-2} s^{-1}):

$$R_o = K_o + L_o. \tag{1}$$

[11] With no change in the amount of the overlying sky view obscured by surrounding topography, adjustment of level R_o for slope effects is made by the following correction of direct-beam shortwave irradiance (K_b)

$$R_o(S) = \omega K_b + K_d + L_o, \tag{2}$$

where $R_o(S)$ is the all-wave irradiance to the slope, K_d and L_o are the respective nondirectional fluxes of diffuse shortwave and longwave irradiance; the geometric slope correction factor ω (dimensionless) scales direct-beam shortwave irradiance from a horizontal surface to a sloped surface by the following ratio:

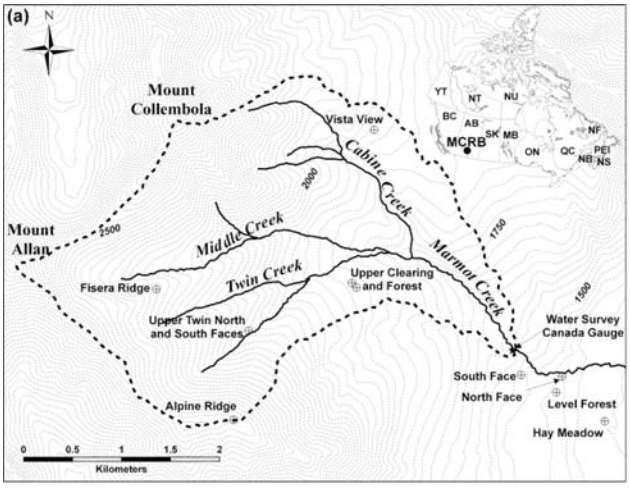

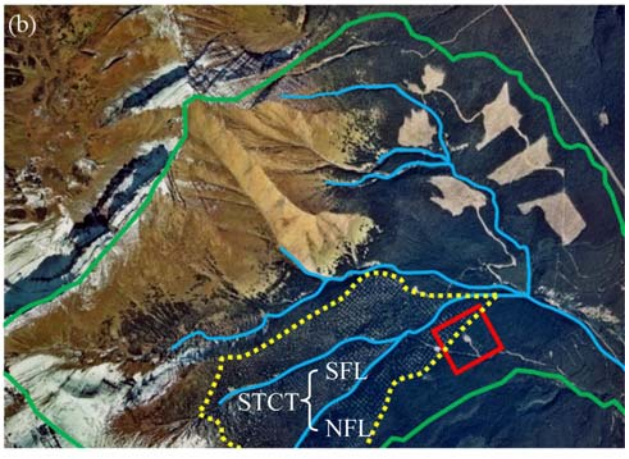

Figure 1. (a) Map of MCRB showing the main subbasins and stream channel network, (b) aerial photograph MCRB showing the general location of the honeycomb patterned forest gap-thinning treatment of small circular gaps along opposing slopes of the north and south Twin Creek tributaries (yellow dashed line) and the NFL and SFL of the STCT used for simulations in section 6, (c) a close-up of forest gaps in the red outlined inset in Figure 1b.

$$\omega = \frac{\cos(Z_S)}{\cos(Z)}, \tag{3}$$

where Z and Z_S are the angles between the direct-beam sky position to the zenith of a horizontal and sloped site, respectively (radians).

3.2. Irradiance to Forest Snowcover

[12] Under a forest canopy of assumed homogenous and isotropic spatial distribution, irradiance to subcanopy snowcover ($R_{\text{in},f}$) is resolved through separate treatment of shortwave and longwave fluxes by

$$R_{\text{in},f} = \omega K_b \tau_b + \tau_d (K_d + L_o) + (1 - \tau_d)\varepsilon_f \sigma T_f^{\,4}, \quad (4)$$

where τ_b and τ_d are the respective forest transmittances of beam and diffuse irradiance (both dimensionless), σ is the Stephan-Boltzmann constant (W m^{-2} K^{-4}), and ε_f and T_f are the respective thermal emissivity (dimensionless) and temperature (K) of forest cover. In equation (4), τ_b may be approximated through sloping forest canopy by

$$\tau_b = e^{-\frac{L'}{\omega \sin(\theta)}}, \quad (5)$$

where L' is the optical depth of the canopy (dimensionless) which is equal to the negative logarithm of irradiance transmission through a vertical profile of the forest layer [*Ellis*, 2011], and θ is the solar elevation angle (radians).

3.3. Irradiance to Forest Gap Snowcover

[13] Using a similar convention to that for open and forest sites above, irradiance in a forest gap is determined by an adaptation of the *Lawler and Link* [2011] geometric model. Here, the forest gap is abstracted as an upright circular opening of a diameter/height dimension equal to d/h, for which irradiance to the center of the gap base ($R_{\text{in},g}$) is given by the following expansion of equation (4)

$$R_{\text{in},g} = \omega K_b \tau_{b,g} + V_{\text{gap}}(K_d + L_o) + \left(1 - V_{\text{gap}}\right)\left[\tau_d (K_d + L_o) + (1 - \tau_d)\varepsilon_f \sigma T_f^{\,4}\right], \quad (6)$$

where $\tau_{b,g}$ is the transmittance of direct-beam irradiance through the surrounding forest cover (dimensionless), and V_{gap} is the fraction of the overlying hemisphere opened to the base of the gap which is determined using the following expression derived from the following geometric view factor for an upright cylinder developed by *Leuenberger and Person* [1956] and *Buschman and Pittman* [1961]

$$V_{\text{gap}} = 1 - \frac{2h}{d}\left\{\left[1 + \left(\frac{h}{d}\right)^2\right]^{1/2} - \frac{h}{d}\right\}. \quad (7)$$

[14] It must be noted that determinations of V_{gap} by expressions such as equation (7) are strictly valid only for horizontal sites. However, analytical expressions for slopes have not yet been developed. To evaluate the error in V_{gap} determinations using equation (7), Appendix A compares values for a horizontal site to sites of increasing slope gradient calculated using a numerical solution approach. Results in Appendix A show that notable differences in V_{gap} values occur only for more open forest gaps (i.e., $d/h > 5$) which are much wider than the forest gaps at the MCRB (i.e., $d/h < 1\frac{1}{4}$), and therefore the use of equation (7) is justified for this study.

[15] In equation (6), $\tau_{b,g}$ is calculated with account for the reduced extinction pathlength by presence of the gap via γ in the following modification of equation (5)

Table 1. Period of Array Irradiance Observations Collected at Paired "Small" Gap-Forest Sites and "Large" Gap-forest sites, Stating the Diameter-to-Height Ratio (d/h) of the Gap Sites, and Canopy Transmittance of Diffuse Shortwave Irradiance (τ_d) Used for Simulations[a]

Site	Period of Observation	d/h[b]	τ_d[c]
"Small" Gap Site	DOY 73–75	0.9	0.14
"Small" Forest Site	DOY 73–75		0.14
"Large" Gap Site	DOY 76–78	3.8	0.18
"Large" Forest Site	DOY 76–78		0.18

[a]Note that gap τ_d values are specified to be equal to those for the corresponding forest site.
[b]In reference to the center of the gap site.
[c]As estimated from manual forest mensuration surveys.

$$\tau_{b,g} = e^{-L'\gamma}, \quad (8)$$

in which γ (dimensionless), with adjustment for slope effects by ω, is given by the following adaptation of T. Link's (Radiation regimes in discontinuous forest canopies: evidence for incoming all–wave radiation paradoxes, in preparation, 2012) formulation

$$\gamma = \frac{1}{\omega}\left(\sin^{-1}(\theta) - \frac{d}{2h}\cos^{-1}(\theta)\right). \quad (9)$$

4. Evaluation of Irradiance Simulation in Gap and Forest Sites

[16] To validate the procedure outlined above, simulations of irradiance were compared to observations collected in paired forest and gap sites located approximately 15 km south of the MCRB over a 5 day period in March 2006 under predominantly clear-sky conditions. Observations of shortwave irradiance (K_{in}) and longwave irradiance (L_{in}) were made in a (i) "small" forest gap site ($d/h \sim 1$) and an adjacent forest site in the surrounding forest cover, as well as in a similarly paired (ii) "large" forest gap site ($d/h \sim 4$) and adjacent forest site. All sites were located on generally level terrain. Physical descriptions of both the small and large paired *gap-forest* observation sites are given in Table 1. At both paired sites, irradiance was measured by two arrays consisting of 10 pyranometers and 12 pyrgeometers, of which individual shortwave and longwave sensors were co-located (except for the two extra pyrgeometers) along a north-south transect spanning the gap opening and extending into the adjacent forest. Irradiance was observed over 2 days in the "small" gap-forest sites followed by 3 days in the "large" gap-forest sites where measurements were acquired at a sampling frequency of 5 s, which were subsequently averaged and recorded at 15 min intervals. Similarly, model simulations at each of the gap-forest sites were performed on a 15 min time step using forcing data of shortwave irradiance (K_o) and longwave irradiance (L_o) collected by the single pyranometer-pyrgeometer sensor pair at the nearby open site. Forest temperatures (T_f) were specified in the model using canopy temperature measurements from an infrared thermometer.

[17] Comparison of simulated irradiance to observations at each of the "small" gap-forest sites and the "large"

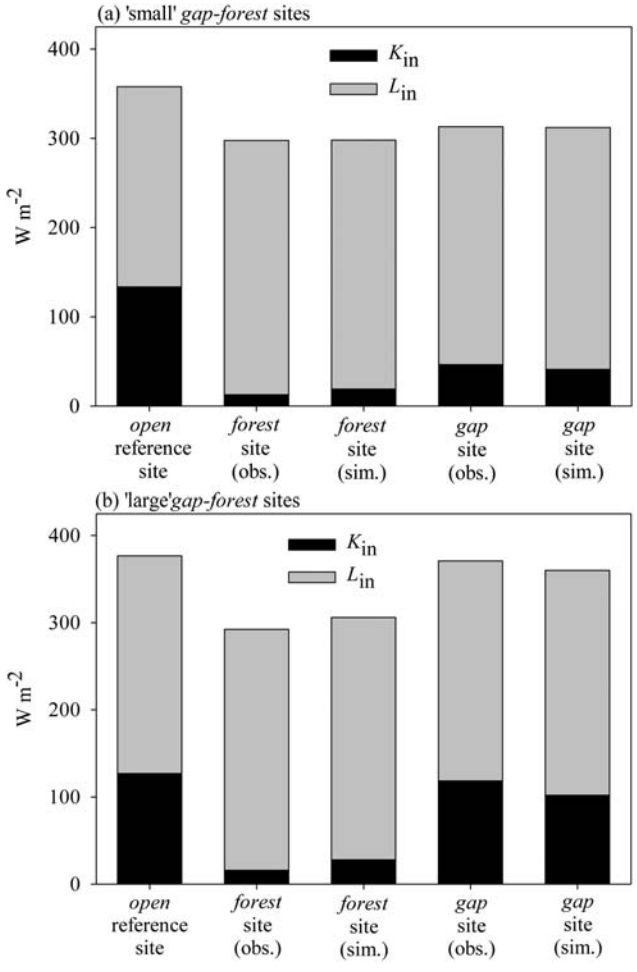

Figure 2. Comparison of mean daily observed and simulated all-wave irradiance to snow (R_{in}), showing the relative contributions of shortwave irradiance (K_{in}) and longwave irradiance (L_{in}) at (a) the "small" paired gap-forest sites, and (b) the "large" paired gap-forest sites. Also shown for Figures 2a and 2b are the corresponding irradiances observed at a nearby open reference site.

gap-forest sites is provided in Figure 2 in terms of the mean total irradiance (R_{in}) and the relative contributions provided by shortwave irradiance (K_{in}) and longwave irradiance (L_{in}). In general, the comparison shows that model simulations well represent the observed variation in total R_{in} among the sites, as well as the sizeable differences in K_{in} and L_{in} contributions to R_{in} between gap and forest sites. As expected, K_{in} is much reduced and L_{in} is increased under forest cover relative to that at the corresponding gap and open sites. The largest differences between gap and forest irradiance occurs in the "large" paired sites (Figure 2b), where both K_{in} and R_{in} in the gap well exceed that in the forest. In contrast, the smaller relative increase in K_{in} in the "small" gap is largely offset by an increased subcanopy L_{in} in the adjacent forest, resulting in comparatively similar R_{in} magnitudes between these gap and forest sites. Note that the slight deviation in open irradiance values between the "small" and "large" site simulations results from the differing time periods of observation.

[18] As stated in section 3, simulations of gap direct-beam shortwave irradiance and longwave irradiance are made in reference to the center of an abstracted circular forest gap opening, and therefore does not explicitly account for the spatial variability in K_{in} and L_{in} observed across both the "small" and "large" gaps. It is also important to note that these comparisons are made over only a few days in March which casts uncertainty of how well the model will perform during later spring melt periods. To address this uncertainty, the model is further evaluated against spatially distributed simulation outputs by *Lawler and Link* [2011] at University of Idaho Experimental Forest (47°51′N, 116°43′W) for the months of February to May in forest gaps with opening sizes (d/h) ranging from 1 to 6. These comparisons show that for small forest gaps (i.e., $d/h = 1$) at this lower-latitude site, center-point simulations compared relatively well for the months of February and March (i.e., <1% underestimation by the center-point model) with differences increasing into April and May (i.e., ~10% overestimation by the center-point model for May). Greatest differences between simulations occurred during April and May in medium-sized gaps (i.e., $d/h = 2 \rightarrow 4$) where the single-point model overestimated the distributed simulation by up to 16%. These results indicate that while center-point simulations may provide reasonably good approximations of mean irradiance for small forest gaps (i.e., $d/h = 1$), considerable uncertainty exists in the reliability of simulations in larger forest gaps, particularly at lower latitudes during later spring periods when solar elevations are higher.

5. Local-Scale Simulation of Snow Accumulation and Melt in Gap and Forest Sites

[19] The gap and forest radiation estimation procedures outlined in section 3 and evaluated above were incorporated into the mass and energy balance routines of the Cold Regions Hydrological Modeling (CRHM) Platform [*Pomeroy et al*., 2007]. CRHM is a modular modeling system designed for cold regions that includes modules to quantify shortwave and longwave radiation fluxes in complex-vegetated terrain, wind redistribution of snow, snowcover energetics, infiltration into frozen and nonfrozen soils, soil drainage, evapotranspiration, and basin scale routing. Figure 3 provides a general schematic of the coupled radiation model — CRHM module configuration used for simulating snow processes in gap and forest sites. As shown by this schematic, snow redistribution is the principal difference in how gap and forest sites are treated by the coupled model; snowfall is allowed to fall directly to the ground without redistribution in gap sites, but is subject to canopy interception and sublimation losses in the forest sites as calculated by the canopy mass and energy balance routines outlined by *Ellis et al*. [2010].

[20] To assess the effectiveness of the coupled radiation-CRHM model for determining snow accumulation and melt in gap and forest sites, simulations of snow water equivalent (SWE) were compared to observations collected at paired gap and forest sites located along the opposing generally north facing and south facing slopes of the south Twin Creek tributary (STCT). Here, the opposing gap sites are small single circular forest openings ($d/h \sim 1$) cut

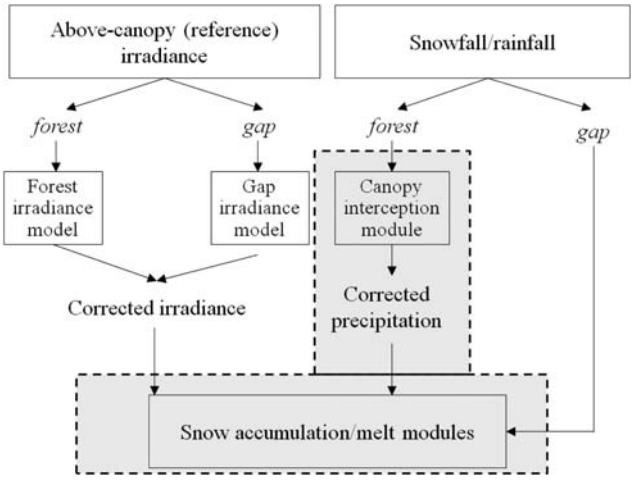

Figure 3. General model configurations for simulation of snow accumulation and melt at gap and forest site types showing the linking of the respective irradiance simulations to the mass and energy balance calculation modules of the Cold Regions Hydrological Model (CRHM). CRHM modules are shown in grey dashed outlines.

within the spruce-dominated forest cover to form part of the honeycomb patterned gap thinning treatment (Figure 1b), with the corresponding forest sites located under the remnant forest cover between the gaps. For clarity, these observation sites are referred to as the (i) north facing forest site (NF), the (ii) north facing gap site (NG), the (iii) south facing forest site (SF), and the (iv) south facing gap site (SG), and are described in Table 2 in terms of general topography as well as forest cover characteristics as determined from forest mensuration and analysis of hemispherical imagery.

[21] At each of these sites, SWE was measured throughout the winter by manual surveying of snow depth and density along established north-south transects, which were repeated approximately every 2 weeks prior to melt and every 2 to 3 days during melt. By relating survey snow depths to measurements provided by an automated ultrasonic depth sensor at each forest site a continuous data set of area-averaged snow depth was established from which a corresponding SWE data set was produced by the linear interpolation of snow density values over the winter.

Table 2. Topography and Forest Cover Characteristics of Forest and Gap Observation Sites in the STCT, where LAI′ is the Leaf Area Index Effective for Snow Interception, τ_d is the Canopy Transmittance of Diffuse Shortwave Irradiance, and *d/h* is the Diameter-to-Height Ratio of the Gap Site

Site	Elevation (m.a.s.l.)	Slope/ Aspect (°/°)	LAI′ (m^2/m^2)	τ_d	*d/h*
North facing Forest Site (NF)	2024	28/330	2.3	0.21	
South facing Forest Site (SF)	2021	26/164	2.5	0.19	
North facing Gap Site (NG)	2028	29/330	0[a]	0.21[b]	1.3
South facing Gap Site (SG)	2016	27/164	0[a]	0.19[c]	1.1

[a]In reference to the center of the gap site.
[b]τ_d of forest cover surrounding the gap site is set equal to that at the corresponding forest site.
[c]As estimated from hemispherical photograph analysis.

[22] For the simulation of SWE at each observation site, forcing data sets of above-canopy irradiance and precipitation were prepared by adjusting observations collected in a nearby forest clearing located approximately 1.5 km northeast and 70 m lower in elevation (Upper Clearing site in Figure 1a). Precipitation corrections for elevation were made using standard lapse rate corrections and radiation adjustments by geometric corrections [*Pomeroy et al.*, 2007]. Model forcing data of air temperature, wind speed, and relative humidity were provided from near-surface observations collected at the forest sites, which were also used for simulations at the corresponding gap sites. Although greatest errors in using forest meteorological conditions to proxy gap conditions are expected for near-surface wind speeds, measurements from a portable anemometer revealed gap wind speeds to be low and similar to those under the forest canopy (differences < 0.3 m s^{-1}) which is attributed to the high degree of wind sheltering from the small openings of both gap sites. Finally, to provide a common specification of forest cover density for the simulation of radiation transfer and interception processes, the canopy transmittance of diffuse irradiance (τ_d) in section 3 was related to a leaf area index effective for interception (LAI′) through the following modification of *Pomeroy et al.*'s [2002] expression:

$$LAI' = e^{-\frac{(\tau_d - 0.45)}{0.29}}. \quad (10)$$

[23] Using the modeling framework established above, time series simulations of SWE at the forest and gap sites are shown compared to observations over the 2008 period of snowpack warming and melt (i.e., day of year (DOY) 90–150) in Figure 4. Here, a marked difference in snow accumulation is evident between the gap and forest sites as canopy interception losses over the winter reduce forest accumulations to nearly half of those in the gaps. Although model simulations are seen to generally capture the pronounced differences in both snow accumulation amounts and melt timing between sites, a more formal evaluation of model performance is made by the following statistical measures: the mean (or model) bias (MB) index, the model

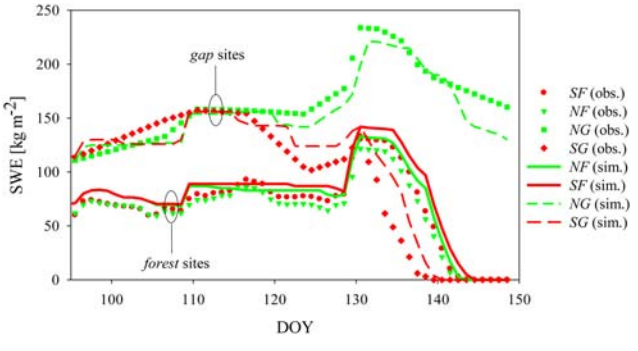

Figure 4. Time series of simulated and observed SWE at the north facing forest site (NF), the south facing forest site (SF), the north facing gap site (NG), and the south facing gap site (SG) of the STCT over the period of spring snowpack warming and melt (i.e., DOY 90–150). Ovals indicate a reference to multiple individual plots.

efficiency (ME) index, and the root mean square error (RMSE), which are determined respectively by

$$\mathrm{MB} = \frac{\sum_{i=1n} x_{\mathrm{sim}}}{\sum_{i=1n} x_{\mathrm{obs}}}, \tag{11}$$

$$\mathrm{ME} = 1 - \left[\frac{\sum_{i=1n} (x_{\mathrm{sim}} - x_{\mathrm{obs}})^2}{\sum_{i=1n} (x_{\mathrm{obs}} - x_{\mathrm{avg}})^2}\right], \tag{12}$$

$$\mathrm{RMSE} = \sqrt{\frac{1}{n}\sum_{i=1}^{n} (x_{\mathrm{sim}} - x_{\mathrm{obs}})^2}, \tag{13}$$

where x_{sim} and x_{obs} are the simulated and observed daily SWE values for a total of n number of paired values, and x_{avg} is the average value of observations. Accordingly, MB values < 1 signify an overall under-prediction by the model and values > 1 an overall overprediction by the model. For the ME index, good model performance is indicated for values approaching 1; 0 indicates an equal efficiency between simulations and the x_{avg}, and increasingly negative values signify progressively poorer model performance. In addition, the RMSE provides a quantification of the amount of unit error between daily x_{sim} and x_{obs} values.

[24] MB, ME, and RMSE index values were used to evaluate the simulation of daily SWE at each site over the period of snowpack warming and melt (i.e., DOY 90–150) and are stated in Table 3. A slight systematic underestimation of SWE at the NG site over the period is indicated by a $\mathrm{MB} < 1$, with overestimation of SWE at all other sites, among which a maximum systematic bias of 17 % (i.e., $\mathrm{MB} = 1.17$) was attained at the NF. Due to shallower subcanopy snow accumulations, simulation errors in terms of absolute unit error (i.e., RMSE) were less at the forests compared to the gaps, being greatest at the NG site where snow accumulation was the deepest. Overall, generally high ME values (0.69–0.89) were obtained for all sites, indicating that model simulations well represented the observed variation in daily SWE values at each site throughout the period.

[25] In addition to snow accumulation differences, Figure 4 also reveals the strong influence forest cover has on the timing of snowmelt between sites. Unlike the forests where a close correspondence in melt timing exists, a pronounced divergence in timing occurs between the opposing gaps, with earlier and more rapid melt at the south facing SG and much slower melt at the north facing NG where a substantial snowpack persists to the end of the period on DOY 149 (snow surveys were terminated on DOY 149 for logistical reasons). To provide a more detailed assessment of the combined effects that forest cover and slope orientation have on snowmelt timing, the snowmelt energy (Q_M) balance at each site was examined as determined by the CRHM Energy Balance Snowmelt Module (EBSM) via

$$Q_M = Q_K + Q_L + Q_H + Q_E + Q_G + Q_P - \frac{\mathrm{d}U}{\mathrm{d}t}, \tag{14}$$

where $\mathrm{d}U/\mathrm{d}t$ is the change in internal (stored) energy of snow, Q_K and Q_L are net shortwave and longwave radiation fluxes, respectively, Q_H and Q_E are the net sensible and latent heat turbulent fluxes, respectively, Q_G is the net ground heat flux, and Q_P is the energy from rainfall advection (all units W m^{-2} or MJ m^{-2} s^{-1}).

Table 3. Determined MB Index, ME Index, and RMSE for Model Simulations of Daily SWE at the Paired STCT Forest and Gap Observation Sites Over the Snowpack Warming and Melt Period (DOY 90–150)

Site	MB	ME	RMSE (kg m^{-2})
North facing Forest Site (NF)	1.17	0.69	5.2
South facing Forest Site (SF)	1.10	0.75	6.1
North facing Gap Site (NG)	0.95	0.89	21.5
South facing Gap Site (SG)	1.08	0.88	15.8

[26] Analysis of equation (14) for the coupled radiation-CRHM snowmelt simulations in Figure 4 reveal that at all the forest and gap sites radiation fluxes dominate total snowmelt energy (Q_M) as simulated turbulent exchanges to snow were limited by the low wind speeds, and only minor energy contributions were provided by ground heat (Q_G) or rainfall advection (Q_P). Among all sites, the highest Q_M occurs at the south facing SG due to large Q_K gains from the direct penetration of shortwave irradiance into the south facing gap. However, Q_L also provides considerable contributions to Q_M at the SG via longwave emissions from the surrounding trees, which act to minimize the negative Q_L balances prior to melt and enhance Q_L gains during melt when longwave losses from snow are limited by a maximum radiating temperature of 0°C. Together, these shortwave and longwave radiation gains are sufficient to facilitate the comparatively early and rapid snowmelt observed at the SG. In contrast to the SG, much lower Q_K contributions are received by snow in the north facing gap (NG) as the site's orientation away from the sun decreases incident shortwave irradiance and its penetration inside the gap opening. With a reduced shortwave flux to snow, combined with the substantial longwave losses from exposed gap snow to the above atmosphere, a large snowpack energy deficit accumulates throughout the winter to create a "cold (radiation) hole" in the NG [*Bernier and Swanson*, 1993]. This sizeable winter energy deficit results in delayed snowmelt which, when occurs, is facilitated mostly by longwave gains from surrounding canopy emissions upon air temperatures warming above freezing.

[27] In contrast to the gap sites, snowmelt energy (Q_M) at both forest sites is dominated by longwave radiation (Q_L) as the dense spruce canopy restricts shortwave irradiance to snow and largely masks the topography-controlled shortwave differences between north facing and south facing slopes. As a result, snowmelt timing is closely synchronized between the opposing forested slopes, with rapid melt at both forest sites proceeding upon above-freezing air temperatures when canopy longwave gains exceed the restricted longwave losses from 0°C snow.

[28] Considering the good model simulations of snow accumulation and melt timing at all forest and gap observation sites, differences in simulated snowmelt energy balances strongly suggest the need for accurate representation of both slope orientation and forest cover effects in predicting snowmelt in complex mountain forest environments. The

benefit of incorporating a more realistic description of radiation dynamics in determining snowmelt in gap-thinned forests is further demonstrated by the much degraded estimation of snowmelt at gap sites for which simulations were performed with the complete removal of surrounding forest cover (i.e., snowmelt in a gap site was simulated as if it were an open site). Simulations of gap sites as open sites produced much lower ME values of 0.52 and 0.21 at the south facing SG and north facing NG sites, respectively. Such results illustrate the unique and disparate radiation environments that may be created in forest gaps compared to open or forest environments, and demonstrates the need for the separate characterization of these three sites types in modeling approaches.

6. Model Application: Impacts of Gap-Thinning Treatments on Snowmelt Across Mountain Landscapes

[29] Following the above site-scale simulations of snow accumulation and melt energetics at the gap and forest sites, the model is further applied in this section to investigate the impacts of the gap-thinning treatments on snowmelt across the STCT of the MCRB. For this exercise, the previous point-scale simulations are expanded to encompass the entire original north facing landscape (NFL) and south facing landscape (SFL) areas in the STCT on which the gap-thinning treatments were performed (NFL and SFL shown in Figure 1b). On both the NFL and SFL, model simulations of snow accumulation and melt were completed over the 2007–2008 winter period, which was generally characterized by steady snow accumulation throughout the winter punctuated by a large snowfall in early May. Simulations on both the NFL and SFL were made with the following two cover types: (i) intact forest cover of the same canopy-cover radiation transfer and interception characteristics specified for point-scale simulations, and (ii) *gap-thinned* (or *gap-thinning*) cover, composed of intact forest patterned with small circular gaps (i.e., $d/h = 1$). For these simulations, gap-thinned covers are intended to represent the forest gap-thinning treatment performed across the STCT, in which approximately 60% of the forest covered area was replaced by small gap clearings. Accordingly, SWE in the gap-thinned covers is determined by the model as the sum of forest and gap site accumulations weighted by their respective 40% and 60% areal coverages.

[30] To illustrate the potential range of snowmelt responses from the gap-thinning treatments across the STCT, Figure 5 shows the simulated snowmelt for varying configurations of intact forest and gap-thinned covers assigned to the opposing NFL and SFL slopes of the tributary. Similar to the previous point-scale simulations, the tributary's general topographic orientation results in the gap-thinning treatment having disparate effects on snowmelt timing between the NFL and SFL by delaying melt in the former and advancing melt in the latter, resulting in a substantial expansion of the snowmelt period. Consequently, when applied across the entire STCT, the gap-thinning treatment results in a substantial divergence in snowmelt timing on the opposing slopes compared to the closely synchronized melt when the tributary is covered by intact forest cover.

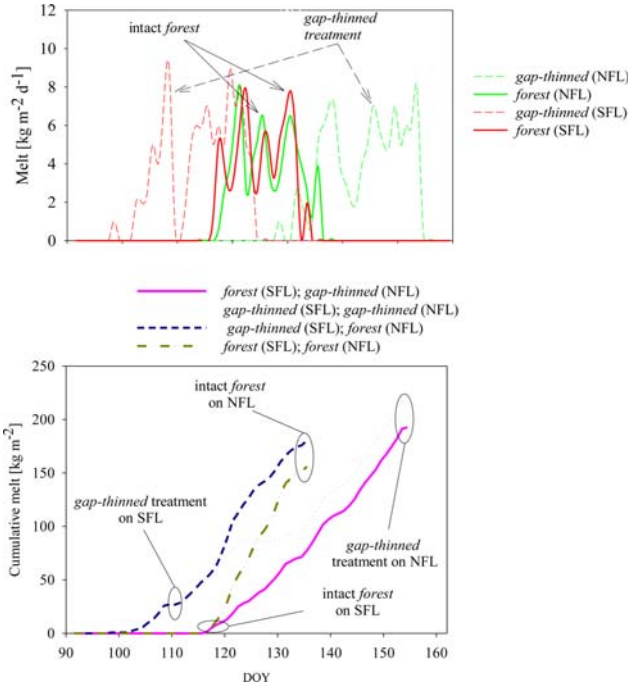

Figure 5. (top) Simulated daily snowmelt and (bottom) corresponding cumulative snowmelt for differing configurations of (i) intact forest and (ii) gap-thinned covers on the NFL and SFL of the STCT. Ovals indicate a reference to two individual plots.

[31] Due to the opposing effects the gap-thinned treatments have on the timing of snowmelt between the NFL and SFL slopes, a large range in spring snowmelt responses may be realized in the STCT through differing cover-topography configurations across the tributary. This is shown in Figure 5 (bottom) by the large divergence in the timing of cumulative melt for differing cover scenarios across the STCS during the spring of 2007–2008. Again, the presence of the gap-thinned treatment across the tributary acts to greatly lengthen the total spring snowmelt period, but also substantially increases the total snowmelt due to deeper winter snow accumulation in the gap-thinned covers. In addition, substantial shifts in snowmelt timing occur with the introduction of the gap-thinned cover, which serves to delay NFL snowmelt and advance SFL snowmelt by up to 20 days for the simulation period.

[32] The influence of tributary (or valley) orientation on the impact the gap-thinned treatments have on snowmelt may be further demonstrated through a 90° horizontal rotation of the STCT, resulting in a hypothetical tributary composed of generally opposing east facing landscape (EFL) and west facing landscape (WFL) slopes. As expected, CRHM simulations over this reoriented tributary show similar cumulative snowmelt amounts for the same cover-topography configurations. However, in terms of snowmelt timing across the reoriented tributary, replacement of intact forest cover with gap-thinned cover results in a similar delay of snowmelt on both the EFL and WFL (Figure 6). This modest response in snowmelt timing to changes in forest cover occurs as the reorientation of the tributary acts to minimize topography-controlled differences in shortwave

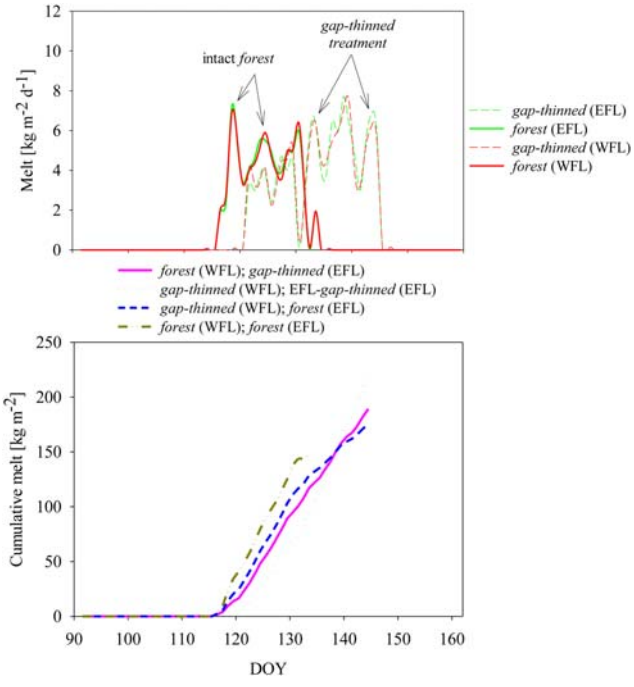

Figure 6. (top) Simulated daily snowmelt and (bottom) corresponding cumulative snowmelt for differing configurations of (i) intact *forest* and (ii) *gap-thinned* clear-cut treatments on the EFL and WFL of a hypothetical 90° rotated STCT.

irradiance in the gap-thinned landscape where snowmelt energy is slightly less than under forest cover due to reduced longwave inputs from the canopy. As a result, the potential variation in snowmelt timing under differing forest and gap-thinned landscape scenarios is much reduced for the reoriented tributary with east facing and west facing slopes compared to the original tributary orientation with south facing and north facing slopes.

7. Snowmelt Sensitivity to Meteorological Conditions

[33] One advantage particular to physically based modeling approaches lies in the ability to examine how physical processes such as snowmelt respond to varying meteorological forcings and snowcover conditions. From this, simulation results may be assessed across a greater range of seasonal conditions, thus extending the results obtained previously over a single winter season. For this analysis, the sensitivity of snowmelt timing and melt energetics was assessed for the following shift in meteorological forcings:

[34] A systematic shift in air temperature of $\pm 1^{\circ}$C, $\pm 2^{\circ}$C, and $\pm 3^{\circ}$C relative to that observed over the 2007–2008 season at the upper-clearing reference site (note that air vapor pressures are held constant for simulations). Due to the strong relation between air temperature and atmosphere, canopy, and snow temperatures, air temperature shifts are intended to illustrate the effect of changing longwave dynamics on snowmelt.

[35] Alternatively, the impacts of varying snowcover conditions are assessed in terms of:

[36] An adjustment in snow albedo (α_s) of ± 0.02, ± 0.04, and ± 0.06 relative to that simulated under observed meteorological conditions for the 2007–2008 season. Consequently, shifts in α_s values are intended to directly represent albedo effects on shortwave gains to snow with varying amounts of snowfall and hence albedo refreshment through the winter. This test also indirectly represents variations in incoming shortwave irradiance via changing cloud cover.

[37] For these specified adjustments, snowmelt timing responses are shown in Figure 7 in terms of (i) the day (DOY) of the median spring snowmelt value and (ii) the corresponding shifts in the snowmelt energy terms in equation (14). Simulations were performed for the previously defined forest and gap-thinned cover as well as on completely open covers (i.e., completely without forest cover) across both the STCT as a whole and on the individual NFL and SFL slopes. For this exercise, shortwave irradiance was approximated using adjusted field observations while sky longwave irradiance was simulated to account for effects of shifting air temperatures for which the sky emissivity with changing cloud cover was estimated following the procedure outlined in *Ellis* [2011].

[38] As shown in Figure 7, seasonal air temperature adjustments prescribed in shift (1) above produce the greatest shifts in snowmelt timing with intact forest cover on the NFL and SFL, which are caused primarily by changes in longwave radiation melt energy (Q_L) due to the relation between air temperature and canopy longwave emissions. However, considerable shifts in melt timing also occur for gap-thinned landscapes by varying the thermal emissions from the surrounding remnant forest cover and from the sky. Alternatively, snowmelt in open landscapes was the least affected by air temperature shifts where longwave irradiance is received primarily from sky emissions. For all the cover types, higher air temperatures advance the start of snowmelt by accelerating the warming of snow temperatures to 0°C, upon which large Q_L gains and rapid melt rates are promoted by the 0°C restricted longwave losses. Increased air temperatures also result in modest additions of snowmelt energy from rainfall advection (Q_P) due to more total rainfall to snowcover; however, overall contributions from Q_P remain relatively modest even on gap-thinned and open landscapes where more rain falls directly to snow. Similar small responses in snowmelt energy inputs from sensible and latent fluxes were caused by air temperature shifts at all sites due to the relatively low wind speeds.

[39] Compared to snowmelt responses from air temperature shifts, systematic adjustments in simulated snow albedo (α_s) prescribed in shift (2) affect snowmelt exclusively through shifts in shortwave melt energy (Q_K) and as a result exhibit marked differences with respect to both cover type and slope orientation. As expected, snowmelt timing is most sensitive to α_s on the SF open and gap-thinned slopes where shortwave irradiance to snow is greatest, and much less sensitive on NF gap-thinned slopes due to the decreased incident shortwave irradiance and limited shortwave penetration into the north sloping forest gap. Due to the later start of melt in the gap-thinned NFL, there is a much greater separation of melt periods between south facing and north facing gap-thinned slopes compared to the open slopes. By comparison, α_s shifts had much less impact

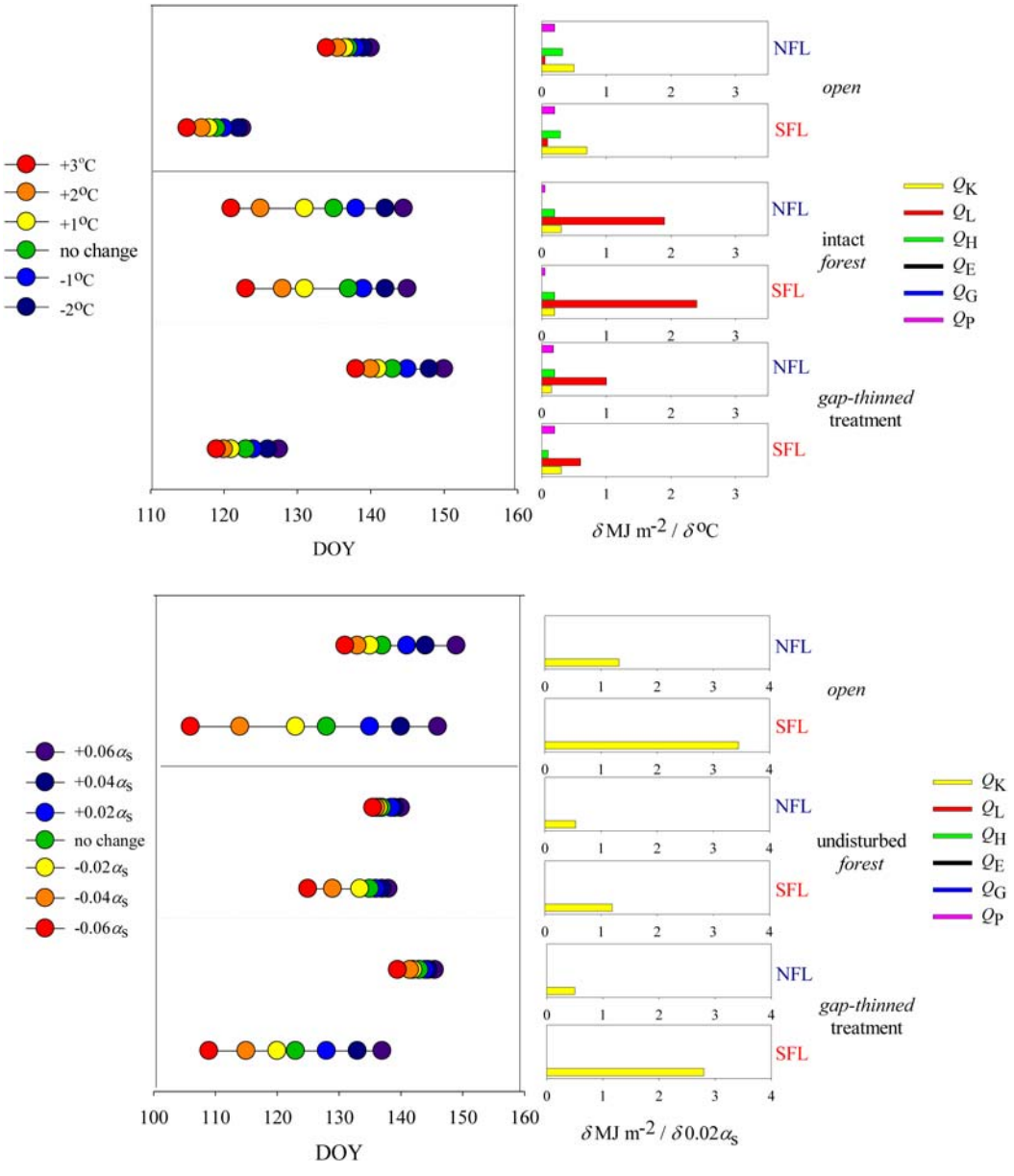

Figure 7. Sensitivity of snowmelt timing and corresponding shifts in melt energy contributions to prescribed shifts in (top) seasonal air temperature (bottom) and snow albedo (α_s) over the 2007–2008 spring melt period for scenarios of (i) open (*ii*) intact forest and (iii) gap-thinned treatments across the NFL and SFL of the STCT. Snowmelt timing is shown in terms of the day of the median snowmelt value.

on snowmelt in intact forest cover irrespective of slope orientation, as forest cover acts to largely mask topography-controlled differences in shortwave irradiance to snow, and by result, Q_K. Consequently, the gap-thinning harvesting treatment across the STCT results in a marked divergence in snowmelt timing between the NFL and SFL landscapes due to the greater shortwave differences created between the opposing north facing and south facing slopes.

8. Discussion

[40] Through the integration of various processes describing canopy interception and snow energetics of cold region forest environments in a common modeling framework, the impact of prescribed forest gap-thinning treatments on mountain snow accumulation and melt was investigated through focused simulations applied in the MCRB, a small headwater basin in the eastern slopes of the Canadian Rocky Mountains. Overall, the coupling of a radiation model developed and tested in small forest gaps with the snow mass and energy balance routines of the Cold Regions Hydrological Model (CRHM) provided a good representation of the considerable differences observed in snowmelt timing between forest gaps on opposing south facing and north facing slopes.

[41] Results from the model application illustrate the marked and varied impacts forest gap-thinning treatments may have upon the spring snowmelt response in mountain

headwater basins. These simulations provided an extension of field-based observations over a larger range of spatial and temporal scales and demonstrated the potential for the gap-thinning treatments across the Twin Creek tributary to alter both the magnitude and timing of spring snowmelt runoff. In terms of water yield, both field observations and simulations indicate a considerable prospect for substantially increasing snow accumulation and spring snowmelt from forest thinning treatments due to reductions in snow interception losses. Alongside snow accumulation effects, of particular interest in the Twin Creek thinning treatment was the promotion of late-season streamflows through delayed snowmelt which was premised on the slower snowmelt rates observed in forest gaps relative to those under nearby forest cover on level terrain [*Troendle and King*, 1985; *Golding and Swanson*, 1986; *Berry and Rothwell*, 1992]. However, both observations and simulations across the STCT demonstrate that snowmelt energetics and resulting melt timing in small forest gaps are strongly influenced by slope orientation. The gap-thinning treatments along the south facing slope of the STCT produced earlier and faster melt due to increased shortwave radiation to snow, while melt was delayed on the north facing slopes due to reduced longwave emission from the canopy. Such disparate effects illustrate the important hydrological control that intact forest cover has in mountain environments through its synchronization of snowmelt across complex terrain.

[42] Although the exact impacts the STCT gap-thinning treatments had on spring streamflow are largely unknown or unreported by previous studies, model results suggest that the expected delay in streamflow would have been substantially moderated as thinning treatments were performed along both the north facing and south facing slopes of the tributary. This is hypothesized as delayed melt on a gap-thinned north facing slope would be expected to be partially offset by the earlier and faster melt on the south facing gap-thinned slope. Alternatively, both field observations and model simulations suggest that delays in snow-derived streamflow would be most effectively gained through gap-thinning treatments targeted exclusively on the north facing slopes of the tributary. These findings strongly suggest that shifts in snowmelt timing brought about by forest cover changes will depend greatly on the slope orientation of the site, the implications of which provides a fundamental advance in the understanding of how vegetation controls the hydrology in cold mountain environments of the higher mid-latitudes. Although some uncertainty remains concerning the accuracy of the radiation and snowmelt simulations in forest gaps using a center-point approximation for gap-integrated radiation, good model evaluation results suggest that the simulations performed should provide a reliable indication of the relative differences in radiation and snowmelt between sites. Robustness of these results is also provided by the similar patterns in snow accumulation and melt timing that have been observed over several winter seasons at the MCRB [*Ellis et al*., 2011]. In addition, results from the model sensitivity analysis revealed that the general pattern of snowmelt responses to forest cover change is maintained across a wide range of seasonal meteorological conditions. Results also reveal the markedly disparate responses in snowmelt timing that may occur between forested and nonforested mountain landscapes resulting from shifts in spring metrological conditions.

9. Conclusions

[43] Findings from both the field observations and model simulations in this study agree with many other investigations reporting canopy thinning resulting in greater snow accumulations. However, the delay of snowmelt in small forest clearings, which has been reported in many level sites, was found only on north facing slopes in the MCRB. Alternatively, the accelerated melt in south facing clearings was more consistent with that found for level sites in Canada [e.g., *Pomeroy and Granger*, 1997]. These results underscore the important role that basin topography and scale of canopy gaps have in determining the effect forest cover changes have on snowmelt energetics and melt timing, with greatest impacts occurring across tributaries of opposing north facing and south facing mountain slopes and relatively little effect across tributaries with opposing east facing and west facing slopes. Further investigation is needed to better understand how forest cover disturbances may affect the timing and magnitude of peak flows from similar mountain regions.

[44] The model applications examined in this study illustrate the considerable potential that forest thinning treatments have toward altering both the magnitude and timing of spring snowmelt response in similar Canadian Rocky Mountain headwater basins. However, uncertainty exists as to what range of environments, elevations, latitudes, meteorological conditions, and seasons these results can be reliably transferred to. For example, at more southerly latitudes, later in the snow season, or on lower slopes, radiation differences between slopes may not be as extreme, but distinct SWE differences may be maintained between forest and gap sites due to greater canopy snow sublimation losses. Similarly, small differences in snowmelt timing may also occur in maritime-dominated climates, where heavy cloud cover reduces shortwave variations across slope and aspect, and where wind effects on turbulent energy transfer rainfall advection may be more responsible for differences between gap-thinned and intact forest covers. While this study provides a fundamental advance in understanding how forest cover physically controls snow processes in areas of complex topography, it also illustrates the complex interplay between forest, snow, and meteorology that requires consideration for properly assessing how changes in forest cover and structure may alter the hydrological response of complex mountain headwater basins.

Notation

CRHM	the Cold Regions Hydrological Model.
d	diameter of forest gap, m.
DOY	day of year.
dt	change in time.
dU	change in internal (stored) energy of snow, MJ m$^{-2.}$
EFL	the east facing sloping landscape area of a 90° reorientated STCT.
h	height of a forest gap, m.
HRU	hydrological response unit.

K_b direct-beam shortwave irradiance, W m^{-2} or MJ m^{-2}.
K_d nondirectional diffuse shortwave irradiance, W m^{-2} or MJ m^{-2}.
K_{in} shortwave irradiance to snow, W m^{-2} or MJ m^{-2}.
K_o shortwave irradiance to level surface, W m^{-2} or MJ m^{-2}.
L' canopy optical depth, dimensionless.
LAI′ leaf area index effective for snow interception, m^2 m^{-2}.
L_{in} longwave irradiance to snow, W m^{-2} or MJ m^{-2}.
L_o longwave irradiance to a level surface, W m^{-2} or MJ m^{-2}.
MB mean (or model) bias index, dimensionless.
MCRB the Marmot Creek Research Basin.
ME model efficiency index, dimensionless.
NF the north facing *forest* site in the STCT.
NFL the north facing sloping landscape area of the STCT.
NG the north facing *gap-thinned* site in the STCT.
Q_E net latent heat snowmelt energy, W m^{-2} or MJ m^{-2}.
Q_G net ground heat snowmelt energy, W m^{-2} or MJ m^{-2}.
Q_H net sensible heat snowmelt energy, W m^{-2} or MJ m^{-2}.
Q_K net shortwave snowmelt energy, W m^{-2} or MJ m^{-2}.
Q_L net longwave snowmelt energy, W m^{-2} or MJ m^{-2}.
Q_M total snowmelt energy, W m^{-2} or MJ m^{-2}.
Q_P net snowmelt energy from rainfall advection, W m^{-2} or MJ m^{-2}.
R_{in} all-wave irradiance to snow, W m^{-2} or MJ m^{-2}.
$R_{in,f}$ subcanopy all-wave irradiance, W m^{-2} or MJ m^{-2}.
$R_{in,g}$ all-wave irradiance in a *gap* site, W m^{-2} or MJ m^{-2}.
RMSE root mean square index, units variable.
R_o all-wave (above-canopy) irradiance to level surface, W m^{-2} or MJ m^{-2}.
$R_o(S)$ all-wave (above-canopy) irradiance to sloped surface, W m^{-2} or MJ m^{-2}.
s second.
SF the south facing *forest* site in the STCT.
SFL the south facing sloping landscape of the STCT.
SG the south facing *gap-thinned* site in the STCT.
STCT the South Twin Creek Tributary.
SWE snow water equivalent, kg m^{-2} or mm.
T_f temperature of forest cover, *K*.
V_{gap} fraction of the overlying hemisphere occupied by a forest gap, dimensionless.
WFL the west facing sloping landscape of the 90° reorientated STCT.
x_{obs} observed value, units variable.
x_{sim} simulated value, units variable.
Z zenith angle of direct-beam irradiance with respect to a horizontal surface, radians.
Z_S zenith angle of direct-beam irradiance with respect to a sloped surface, radians.
α_s snow albedo, dimensionless.
γ gap pathlength correction factor, dimensionless.
ε_f emissivity of forest cover foliage, dimensionless.
θ solar elevation angle above horizon, radians.
σ Stephan-Boltzmann constant, W m^{-2} K^{-4}.
τ_b forest transmittance of direct-beam shortwave irradiance, dimensionless.
$\tau_{b,g}$ gap transmittance of direct-beam shortwave irradiance, dimensionless.
τ_d forest transmittance of diffuse shortwave irradiance, dimensionless.
ω geometric slope correction factor for direct-beam irradiance, dimensionless.

Appendix A: An Assessment of Slope Effects on Forest Gap View Factor (V_{gap}) Determinations

[45] As stated in the manuscript, the determination of the forest sky view factor (V_{gap}) by equation (7) makes the assumption of a horizontal surface. Although, the main focus of this paper is on gaps of relatively small diameter to height ratios (i.e., $d/h < 2$), the assumption of a horizontal surface introduces estimation errors of V_{gap}, particularly in more open gaps. The increasing influence of slope on V_{gap} is shown in Figure A1, which compares determinations of V_{gap} of varying on slopes of varying gradient (dz/dy). Here, slope is seen to have very little influence for relatively closed gaps (i.e., $d/h < 3$), but a progressive divergence in V_{gap} occur with slope for more open gaps (i.e., $d/h > 5$). At maximum, the assumption of a horizontal surface results in an overestimation of V_{gap} of approximately 0.08 (8%) for a slope gradient of 0.7. These results suggest that caution should be taken when applying estimate approaches developed for horizontal on mountain slopes, particularly in more open forest gap environments.

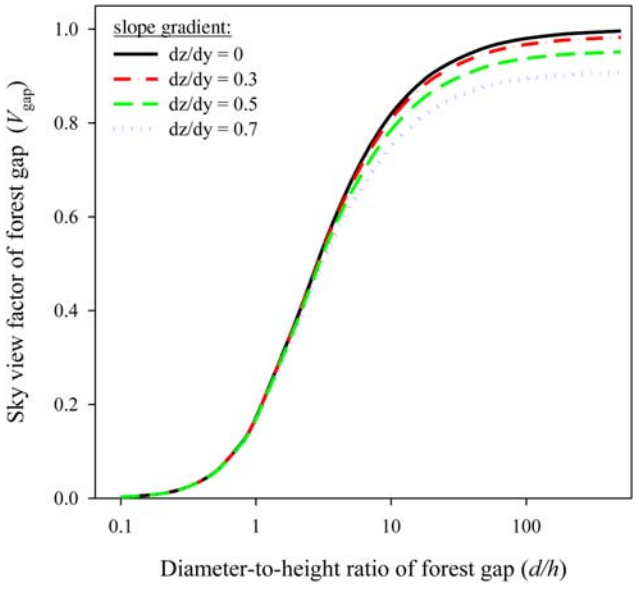

Figure A1. Comparison of determined forest sky view factors (V_{gap}) of varying degrees of openness (d/h) for a horizontal surface and slope gradients (dz/dy) of 0.3, 0.5, and 0.7 (note that graph is based on unpublished data from R. D. Moore).

[46] **Acknowledgments.** The authors first like to thank Dan Moore of the University of British Columbia for the exceptionally thoughtful and thorough review of this paper, which greatly improved its quality. Financial support was provided from the Improved Processes and Parameterization for Prediction in Cold Regions network (IP3) (CFCAS), the NSERC Alexander Graham Bell Scholarships and Michael Smith Foreign Scholarships, and the NSERC Discovery Grants, such as Alberta Sustainable Resource Development and the Canada Research Chairs programme. Field work assistance was provided by Michael Solohub, Anne Sabourin, and students of the Centre for Hydrology. Logistical assistance from the University of Calgary Biogeoscience Institute and Nakiska Ski Area is gratefully appreciated.

References

Barnett, T. P., et al. (2008), Human-induced changes in the hydrology of Western North America, *Science*, *319*, 1080–1083.

Beckstead, G. R. E., and W. M. Veldman (1985), *The Marmot Creek Experimental Watershed: Final Report*, pp. 1–119, HydroCon Eng. (Continental) LTD, Alberta, Canada.

Bernier P., and R. Swanson (1993), The influence of gap size on snow evaporation in the forests of the Alberta foothills, *Can. J. For. Res.*, *23*(2), 239–244.

Berry, G. J., and R. L. Rothwell (1992), Snow ablation in small forest openings in southwest Alberta, *Can. J. For. Res.*, *22*(9), 1326–1331, doi:10.1139/x92-176.

Burles, K., and S. Boon, (2011), Snowmelt energy balance in a burned forest plot, Crowsnest Pass, Alberta, Canada, *Hydrol. Process.*, *25*(19), 3012–3029, doi:10.1002/hyp.8067.

Buschman, A., and C. M. Pittman (1961), Configuration factors for exchange of radiant energy between axisymmetrical sections of cylinders, cones, and hemispheres and their bases, Rep. NASA TN D-944, NASA, Washington DC, USA.

Church, J. E. (1912), The conservation of snow – Its dependence on forests and mountains, *Sci. Am. Suppl.*, *74*(1914), 152–155.

Davis, R. E., J. P. Hardy, W. Ni, C. Woodcock, J. C. McKenzie, R. Jordan, and X. Li (1997), Variation of snow cover ablation in the boreal forest: A sensitivity study on the effects of conifer canopy, *J. Geophys. Res.*, *102*, 29,389–29,395, doi:10.1029/97JD01335.

Ellis, C. R. (2011), Radiation and snowmelt dynamics in mountain forests, Ph.D. thesis, Dep. of Geogr. and Plann., Univ. of Sask., Sask., Canada.

Ellis, C. R., J. W. Pomeroy, T. Brown, and J. MacDonald (2010), Simulation of snow accumulation and melt in needleleaf forest environments, *Hydrol. Earth Syst. Sci.*, *14*, 925–940, doi:10.5194/hess-14-925-2010.

Ellis, C.R., J. W. Pomeroy, R. L. H. Essery, and T. E. Link (2011), Observations of forest cover effects on radiation and snowmelt dynamics in the Canadian Rocky Mountains, *Can. J. For. Res.*, *41*, 608–620, doi:10.1139/X10-227.

Eschner, A. R., R. E. Leonard, and A. L. Leaf (1969), Soil moisture priming, soil temperature and water available for snowmelt runoff, in Proceedings of Eastern Snow Conference, pp. 19–23, Niagara on the Lake, Ont., Canada.

Fang, X., J. W. Pomeroy, C. R. Ellis, M. K. MacDonald, C. M. DeBeer, and T. Brown (2012), Multi-variable evaluation of hydrological model predictions for a headwater basin in the Canadian Rocky Mountains, *Hydrol. Earth Syst. Sci. Discuss.*, *9*, 12,825–12,877, doi:10.5194/hessd-9-12825-2012.

Gary, H. L. (1980), Patch clearcuts to manage snow in lodgepole pine, paper presented at the Symposium on Watershed Management, Am. Soc. of Civil Eng., Boise, Idaho.

Gary, H. L., and C. A. Troendle (1982), Snow accumulation and melt under various stand densities in lodgepole pine in Wyoming and Colorado, in Forest Service Research Note RM-417, pp. 1–7, USDA For. Service, Rocky Mountain For. and Range Exp. Stn., Fort Collins, Colo.

Golding, D. L., and R. H. Swanson (1978), Snow accumulation and melt in small forest openings in Alberta, *Can. J. For. Res.*, *8*, 380–388.

Golding, D. L., and R. H. Swanson (1986), Snow distribution patterns in clearings and adjacent forest,*Water Resour. Res.*, *22*, 1931–1940.

Gray, D.M. and P.G. Landine (1988), An energy budget snowmelt model for the Canadian Prairies, *Can. J. Earth Sci.*, *22*(3), 464–472.

Jeffery, W. W. (1965), Snow hydrology in the forest environment, paper presented at the Workshop Seminar: Snow Hydrology, Univ. of New Brunswick, Canada.

Knowles, N., M. D. Dettinger, and D. R. Cayan (2006), Trends in snowfall versus rainfall in the Western United States, *J. Clim.*, *19*, 4545–4559.

Hardy, J. P., R. E. Davis, R. Jordan, W. Ni, and C. Woodcock (1998), Snow ablation modelling at the stand scale in a boreal jack pine forest, *Hydrol. Process.*, *12*(10/11), 1763–1778.

Helgason, W., and J. W. Pomeroy (2012), Characteristics of the Near-Surface Boundary Layer within a Mountain Valley during Winter, *J. Appl. Meteor. Climatol.*, *51*, 583–597, doi:10.1175/JAMC-D-11-058.1.

Lawler, R. R., and T. E. Link (2011), Quantification of incoming all-wave radiation in discontinuous forest canopies with application to snowmelt prediction, *Hydrol. Process.*, *25*(21), 3322–3331, doi:10.1002/hyp.8150.

Leuenberger, H., and R. A. Person, (1956), Compilation of Radiation Shape Factors for Cylindrical Assemblies, paper no. 56-A-144, Am. Soc. of Mech. Eng., New York.

Lundberg, A., and S. Halldin (1994), Evaporation of intercepted snow, analysis of governing factors, *Water Resour. Res.*, *30*, 2587–2598.

Marks, D., and A. Winstral (2001), Comparison of snow depositions, the snowcover energy balance, and snowmelt at two sites in a semi–arid mountain basin, *J. Hydromet.*, *2*, 213–227.

Martz, L., J. Bruneau, and T. Rolfe (2007), Climate change and water, in South Saskatchewan River Basin Final Technical Report, Final technical note, pp. 1–252, University of Saskatchewan, Saskatoon, Sask.

Metcalfe, R.A. and J.M. Buttle (1995), Controls of canopy structure on snowmelt rates in the boreal forest, in Proceedings of the 52nd Eastern Snow Conference, pp. 249–257, Toronto, Ont., Canada.

Mote, P., Hamlet, A., Clark, M., and D. Lettenmaier (2005), Declining mountain snowpack in Western North America, Bull. *Am. Meteorol. Soc.*, *86*, 36–49, doi:10.1175/BAMS-86-1-39.

Nash, C. H., and E. A. Johnson (1996), Synoptic climatology of lightning-caused forest fires in subalpine and boreal forests. *Can. J. For. Res.*, *26*, 1859–1874.

Pomeroy, J. W., and R. J. Granger (1997), *Sustainability of the western Canadian boreal forest under changing hydrological conditions – I – Snow accumulation and ablation, in Sustainability of Water Resources under Increasing Uncertainty*, edited by D. Rosjberg, et al., pp. 237–242, IAHS Publ. No. 240, IAHS, Wallingford, U. K.

Pomeroy, J. W., and D. M. Gray (1995), Snow accumulation, relocation and management, in NHRI Science Rep. No. 7, Environment Canada, Saskatoon, Sask. (Available from NWRI, Saskatoon).

Pomeroy, J. W., R. Granger, A. Pietroniro, J. Elliott, B. Toth, and N. Hedstrom (1999), Classification of the boreal forest for hydrological processes, in Proceedings of the Ninth International Boreal Forest Research Association Conference, edited by S. Woxholtt, pp. 49–59, Aktuelt fra skogforskningen, Norsk institutt for skogforskning, Norw. For. Res. Institute, Oslo.

Pomeroy, J. W., D. M. Gray, N. R. Hedstrom, and J. R. Janowicz (2002), Prediction of seasonal snow accumulation in cold climate forests, *Hydrol. Process.*, *16*, 3543-3558.

Pomeroy, J.W., R. J. Granger, N. R. Hedstrom, D. M. Gray, J. Elliott, A. Pietroniro, and J. R Janowicz (2005), *The process hydrology approach to improving prediction to ungauged basins in Canada, in Prediction in Ungauged Basins, Approaches for Canada's Cold Regions*, edited by C. Spence, J. Pomeroy and A. Pietroniro, pp. 67–95, Canadian Water Resour. Assoc., Cambridge.

Pomeroy, J. W., D. M. Gray, T. Brown, N. R. Hedstrom, W. L. Quinton, R. J. Granger, and S. K. Carey (2007), The cold regions hydrological model, a platform for basing process representation and model structure on physical evidence, *Hydrol. Process.*, *21*(19), 2650–2667, doi:10.1002/hyp.6787.

Pomeroy, J. W., X. Fang, and C. R. Ellis (2012), Sensitivity of snowmelt hydrology in Marmot Creek, Alberta, to forest cover disturbance, *Hydrol. Process.*, *26*(12), 1891–1904, doi:10.1002/hyp.9248.

Sicart, J. E., J. W. Pomeroy, R. L. H. Essery, J. E. Hardy, T. Link, and D. Marks (2004), A sensitivity study of daytime net radiation during snowmelt to forest canopy and atmospheric conditions, *J. Hydromet.*, *5*, 744–784.

Stewart, R. B., E. Wheaton, and D. L. Spittlehouse (1998), *Climate change: Implications for the boreal forest, in Emerging Air Issues for the 21st Century: The Need for Multidisciplinary Management*., edited by A. H. and L. L. Jones, Air and Waste Manage. Assoc., 86–101, Pittsburgh, Penn.

Storck, P., L. Bowling, P. Wetherbee, and D. Lettenmaier (1998), Application of a GIS-based distributed hydrology model for prediction of forest harvest effects on peak stream flow in the Pacific Northwest, *Hydrol. Process.*, *126)*, 889–904, doi:10.1002/(SICI)1099-1085.

Swanson, R. H., D. L. Golding, R. L. Rothwell, and P. Y. Bernier (1986), *Hydrological effects of clear-cutting at Marmot Creek and Streeter*

Creek Watersheds, in Canadian Forest Service Information Rep. NOR-X-278, North. For. Centre, Alberta, Canada.

Troendle, C. A., and R.M. King (1985), The effect of timber harvest on the Fool Creek watershed: 30 years later, *Water Resour. Res.*, *21*, 1915–1922.

Troendle, C. A., and C. F. Leaf (1980), Hydrology, in An Approach to Water Resources Evaluation of Non-Point Silvicultural Sources (A Procedural Handbook), pp. 111-1–111-173, *chap. III, EPA 60018-80-012*, Environ. Res. Lab., Athens.

Troendle, C. A., and C. F. Leaf (1981), Effects of timber harvest in the snow zone on volume and timing of water yield, paper presented at Interior West Watershed Management Symposium, pp. 231–243, *Coop. Ext.*, Washington State Univ., Pullman, Washington, D. C.

Woo, M. K. (2008), *Cold Region Atmospheric and Hydrologic Studies. The Mackenzie GEWEX Experience*, 481 pp., Springer, Berlin.